Available online at www.sciencedirect.com
ScienceDirect
Scripta Materialia xxx (2015) xxx–xxx
Scripta MATERIALIA
www.elsevier.com/locate/scriptamat

Q1 Homogeneous and ultrafine-grained metal matrix nanocomposite achieved by accumulative press bonding as a novel severe plastic deformation process

Q2 Sajjad Amirkhanlou,[a,b,*] Mostafa Ketabchi,[a] Nader Parvin,[a] Alberto Orozco-Caballero[b] and Fernando Carreño[b]

[a]*Department of Mining and Metallurgical Engineering, Amirkabir University of Technology, Tehran, Iran*
[b]*Department of Physical Metallurgy, CENIM-CSIC, Av. Gregorio del Amo 8, 28040 Madrid, Spain*

Received 17 September 2014; revised 10 December 2014; accepted 12 December 2014

Accumulative press bonding (APB) is proposed as a novel method for inducing severe plastic deformation. This process can produce a homogeneous and ultrafine-grained nanocomposite, which is extremely difficult to obtain by other processes. AA1050/SiC_p nanocomposite with an average grain size of 280 nm and well-developed high-angle grain boundaries (39° average misorientation angle and 82% high-angle boundaries) exhibited the highest tensile strength reported in the literature, i.e. 284 MPa. Theoretical models revealed that the contributions of Orowan and grain refinement strengthening mechanisms to yield strength were 76.6% and 14.8%, respectively.

Keywords: Severe plastic deformation (SPD); Accumulative press bonding (APB); Nanocomposite; Ultrafine-grained microstructure; Analytical methods

It is known that severe plastic deformation (SPD) of bulk metallic materials leads to the formation of nanocrystalline (NC) or ultrafine-grained (UFG) microstructures. The mechanical properties of SPD-processed materials are significantly enhanced compared to those of coarse-grained materials due to extensive grain refinement and increased dislocation densities [1]. In addition, reinforcing NC/UFG structured materials with nanoparticles provides great potential for further improving the mechanical properties. In this paper, accumulative press bonding (APB) is proposed as a novel and unique SPD process in order to obtain homogeneous UFG Al/SiC_p metal matrix nanocomposites (MMNCs).

The materials used in this study were aluminum of commercial purity ⩾99.5% (AA1050) with dimensions of 100 mm × 50 mm × 1.5 mm, and SiC nanopowder with a particle size of 55 nm. Before APB processing, the aluminum was annealed at 623 K for 1 h. Figure 1 presents the APB procedure. This process was performed in two steps to produce Al/2 vol.% SiC_p MMNC. After surface preparation (degreasing with acetone followed by scratch brushing), ultrasonicated SiC nanopowder in acetone was sprayed between two aluminum strips with an air-gun atomizer. Then, the two strips were stacked and bonded together at room temperature, without use of lubricants, via a laboratory hydraulic press machine (Toni Technik Baustoffprüffsysteme GmbH). The press bonding process was carried out with a specific amount of reduction equal to 50%. The deformation process was performed in a simple channel-die, resulting in no lateral/width spreading. After the press bonding, the strips were cut in half and the same procedure was repeated up to five cycles in the first stage. In the second and final stage, the same procedure was repeated again up to 14 cycles without adding SiC nanopowder. The same process was employed for the production of the monolithic aluminum, for which the aluminum strips were processed by APB without adding any SiC nanopowder through the process. Electron backscatter diffraction (EBSD) mapping of the monolithic aluminum alloy and Al/SiC_p nanocomposite were conducted in a JEOL JSM 6500 F field emission gun scanning electron microscope (SEM) operating at 20 kV with a working distance of 15 mm and tilt angle of 70°. The microstructures of the specimens were also characterized by transmission electron microscopy (TEM, JEOL JEM 2000) operating at 200 kV and field-emission scanning transmission electron microscopy (FE-STEM, Hitachi S-4800) operating at 30 kV complemented by energy-dispersive spectroscopy (EDS). The tensile test specimens were machined according to the ASTM E8/E8M standard, oriented along the longitudinal direction (strain rate of 1.6×10^{-1} s^{-1}).

Figure 2 shows the TEM micrographs of pure aluminum after various cycles of APB, taken from the longitudinal direction (LD)–transverse direction (TD) planes. The

Q3 * Corresponding author at. Department of Physical Metallurgy, CENIM-CSIC, Av. Gregorio del Amo 8, 28040 Madrid, Spain. Tel.: +98 911 1511024; fax: +98 21 66405846; e-mail addresses: s.amirkhanlou@aut.ac.ir; s.amirkhanlou @ma.iut.ac.ir

http://dx.doi.org/10.1016/j.scriptamat.2014.12.007
1359-6462/

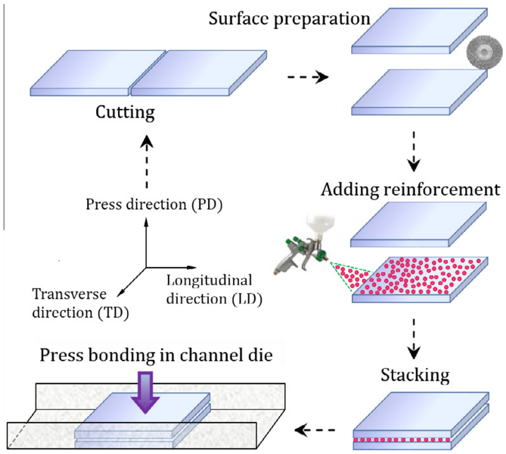

Figure 1. Schematic illustration of accumulative press bonding (APB) process.

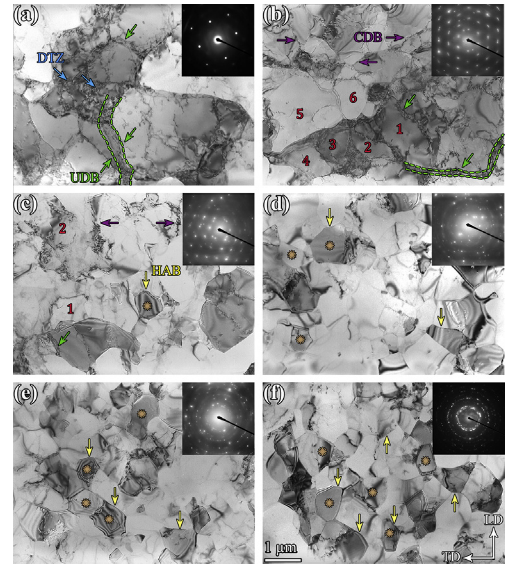

Figure 2. TEM micrographs and corresponding SAED patterns of AA1050 pure aluminum processed by APB after different cycles, taken from the LD–TD planes: (a) 1 cycle, (b) 3 cycles, (c) 5 cycles, (d) 7 cycles, (e) 10 cycles and (f) 14 cycles. The blue arrows mark dislocation tangle zones (DTZs), the green arrows and dashed lines indicate uncondensed dislocation boundaries (UDBs), the numbers denote subgrains, the purple arrows show condensed dislocation boundaries (CDBs), the yellow arrows mark high-angle boundaries (HABs), and the brown stars mark ultrafine grains (UFGs). (For interpretation of the references to colour in this figure legend, the reader is referred to the web version of this article.)

selected-area electron diffraction (SAED) patterns taken from the center of the field, using the largest aperture, are also shown. After one cycle of APB (Figure 2a) the specimen shows a subgrain structure with high dislocation density in the subgrain interiors and dislocation-tangle zones (DTZs). Accordingly, the SAED pattern shows a single net pattern, which confirms that the first cycle results in low misorientation. The specimen after three cycles of APB process (Figure 2b) shows a similar subgrain structure, though the dislocation density and its value within the subgrains has increased and the subgrain size has become finer. Although subgrains are surrounded by uncondensed dislocation boundaries (UDBs) having irregular shapes, these boundaries are much denser than those observed from the one-cycle APB specimen. This indicates that the dislocations are redistributed near the boundaries. Some of these dislocations could form condensed dislocation boundaries (CDBs), as shown in Figure 2b. After five cycles, ultrafine grains with diameters <1 μm and with a new type of boundaries, i.e. high-angle boundaries (HABs), begin to appear, as shown in Figure 2c. After seven cycles of APB (Figure 2d) a UFG structure becomes more dominant and the specimen is covered with ultrafine grains ~700 nm in average size and characterized by clear boundaries. After the 10th cycle, the average grain size is ~550 nm. The SAED patterns also show a more ring-like pattern than those after three or five cycles. In fact, the grain structure of this specimen is nearly the same as that of the seven-cycle specimen except for the shape and size of the ultrafine grains, which are now more equiaxed than in previous cycles. As shown in Figure 2f, after 14 cycles, the specimen presents homogenously distributed ultrafine grains with an average grain size of ~450 nm. The SAED pattern in Figure 2f contains many spots situated around Debye–Scherrer circles indicating the presence of a large number of highly misoriented grains. In summary, Figure 2 provides evidence that there is a sequence of grain refinement when the number of APB cycles, i.e. strain, increases. According to Figure 2, the APB refining mechanism is continuous dynamic recovery characterized by subdivision to ultrafine grains by severe deformation and progressive recovery to form clear ultrafine grains.

EBSD/orientation imaging microscopy (OIM) maps of the initial material and AA1050 pure aluminum processed by APB after different cycles are shown in Figure 3. In all images, the colors within the grains correspond to the orientations of each grain as depicted by the unit triangle at the figure, the grain boundaries shown as gray lines have misorientations (θ) between 2° and 15°, and the boundaries shown as black lines have misorientations of $\theta \geq 15°$. For each specimen, the mean misorientation angle ($\bar{\theta}$) and the fraction of high-angle boundaries (f_{HAB}) are represented in the figure. The fraction of high-angle boundaries is initially low but increases to 63% after five cycles and continues to increase to 78% after 14 cycles. It should be noted that the mean misorientation angle increases with increasing strain during APB and reaches a saturation value of ~34°–35° after 10 cycles. According to the EBSD results, dislocation cells and subgrain structures with low-angle grain boundaries are formed during initial APB cycles. In these initial cycles, due to multidirectional slip, the aforementioned structures became finer. Increasing the number of APB cycles resulted in an increase in the misorientations of the dislocation cell structures and subgrains. Finally, a UFG structure comprised mainly of high-angle boundaries is created. This continuous increase in misorientation during APB resulting in high-angle boundaries is attributed to the rearrangement of the dislocations through short-range diffusion. Therefore, with increasing numbers of cycles, both the average misorientation and the variety of colors in the maps increase.

Figure 4a and b show STEM micrographs of AA1050 pure aluminum and Al/SiC_p nanocomposite processed by APB after 14 cycles, respectively, taken from the press direction (PD)–longitudinal direction (LD) planes. The EDS data taken from the SEM (Figure 4c) confirm that the spherical nanoparticles are SiC. According to Figure 4a, the PD–LD plane of the specimen shows a homogeneous distribu-